A COMPREHENSIVE TOOL TO SIMULATE COMPOSITE LAY-UPS IN PRESSURE VESSELS

L. Bizet, K. Mathis, Philippe Saffré, D. Halm, M. Gueguen, P Francescato, M Jacquesson

A COMPREHENSIVE TOOL TO SIMULATE COMPOSITE LAY-UPS IN PRESSURE VESSELS

L. Bizet [(1)], K. Mathis [(1)], P. Saffré [(2)], D. Halm [(3)], M. Gueguen [(3)], P. Francescato [(2)], M. Jacquesson [(1)]

[(1)] CNES - 52, rue Jacques Hillairet – FR 75012 Paris Cedex, France, Email: kevin.mathis@cnes.fr
[(2)] Univ. Savoie Mont Blanc, SYMME, FR 74000 Annecy, France, Email: philippe.saffre@univ-smb.fr
[(3)] ENSMA - Institut P', BP 40109, F-86961 Futuroscope-Chasseneuil, France, Email: damien.halm@ensma.fr

ABSTRACT

Composite pressure vessels made by filament winding processes are commonly used in aerospace design due to weight saving compared to metal parts. This technique involves complexities in analyzing the geometry especially in the dome section. Tools already exist to predict the geometrical characteristics like winding angle, ply thickness or some singularities. However they are limited to specific sequence dome lay-up. A numerical tool has been developed to simulate windings layer after layer.

The goal is to deal with any kind of sequence dome lay-up calculation. To ensure this there are three main challenges that are seldom cited in scientific literature. The first is when the geometry of the current ply overlaps the inferior ply. The second is the management of convex parts of a ply. Finally, our mathematical tool is able to deal with the accumulation of composite fibers near the polar boss outer radius.

1. INTRODUCTION

The winding process produces composite tanks capable of withstanding high internal pressures. The very high specific properties of these materials lead to structures with remarkable rigidity and strength for a contained mass. The filament winding continuously deposits composite fibers on a mould or a mandrel with a rotational movement. This manufacturing method is particularly suitable for revolution structures. In the space industry this technology is already used for some motor cases or tanks. To best design and optimize these structures it becomes necessary to integrate the simulation of the winding process of composite structures.

The performance of a composite structure depends on the adequacy between the loading directions and the distribution of the fibrous reinforcement. In the case of the filament winding process, a reliable estimation of the mechanical behaviour of the structure is conditioned by the most exact simulation possible of the fiber path, in particular in the domes, considered as the most delicate parts to simulate. Several studies [1-5] have allowed the development of successive winding models that enable the complex geometry of domes to be managed. However, these models remain limited with regard to the strong disparity of possible windings. The objective of this work is to propose a tool for simulating the filament winding of any winding sequences on generic revolution geometries.

The ultimate aim is to use the model developed in an optimization procedure in which lay-up orientation, stacking sequence and filament winding parameters are significant parameters.

2. BASIC ASPECTS

2.1 Winding angle determination

Geodesic winding provides to the best winding stability by finding the shortest fiber path between two points on any surface. However, non-geodesic winding increases the scope of the geodesic winding technique through the use of the slippage tendency of the fibers on their supporting surface.
Descriptions of geodesic and non-geodesic winding methods can be found in [6-8].
For the purposes of future optimization, it is desirable to have a general equation to describe both geodesic and non-geodesic winding. The following equation [7] is valid:

$$\frac{d\alpha}{dz} = \lambda\left[\frac{\sin\alpha\tan\alpha}{r} - \frac{r''}{1+r'^2}\cos\alpha\right] - \frac{r'\tan\alpha}{r} \quad (1)$$

where α is the angle between the fiber tow and the meridian direction of the dome, λ the slippage coefficient of the fiber tows on the supporting surface and *r* and *z* the radial and axial coordinates of the dome, as shown in Fig. 1.
Depending on the sign of λ, the path will be lengthened or shrunk and thus influence the positioning of the radius at the turn-around of the continuous fiber.
Usually this differential equation is solved by a Runge-Kutta method to order 4. The main problem with this method of resolution is the number of integration points required to ensure convergence of results. We will see in the proposed developments that this method of resolution, although used by all the routines allowing the multi-sequence simulation of filament winding, is

not sufficiently adapted due to the inherent nature of the differential equation Eq. 1.

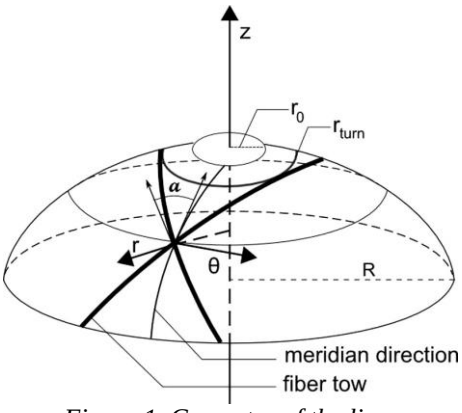

Figure 1. Geometry of the liner

To ensure the continuity of the winding between the cylindrical section of the tank and the dome, the following equation [7] is used :

$$\lambda = \lambda_{max} \cos\left(\frac{\pi}{2}\frac{r - r_{turn}}{R - r_{turn}}\right) \quad (2)$$

where R is the external equator radius of the tank (including the thickness of the plies) in the cylindrical section, r_{turn} the radius at the turn-around point and λ_{max} the arbitrary top value of the slippage coefficient.
The arbitrary top value λ_{max} can be an optimization parameter as long as $|\lambda_{max}| \leq \lambda_{lim}$ where λ_{lim} is the slippage limit coefficient which depends on practical winding parameters.

2.2 Thickness determination

Once the radius at the turn-around point determined by the resolution of Eq. 1, it is necessary to determine the evolution of the thickness of the composite layer of the cylindrical section up to this radius at the turn-around point. Leh [5] presented several formulations of thickness. It shows that Wang's formulation [3] is one of the most recent methods and presents very good results in comparison with the experimental one. It is based on the use of a double formulation to reflect as accurately as possible the thickness evolution:

$$t(r) = \frac{n_R m_R t_p}{\pi}\left[\arccos\left(\frac{r_{turn}}{r}\right) - \arccos\left(\frac{r_b}{r}\right)\right] \quad (3)$$
$$\text{for } r_{2b} \leq r \leq R$$

and

$$t(r) = A + Br + Cr^2 + Dr^3 \quad (4)$$
$$\text{for } r_{turn} \leq r \leq r_{2b}$$

where n_R, m_R are the number of pseudo-plies ($\pm\alpha_R$) and their quantity in the cylindrical section, t_p is the thickness of a fiber tow or tape, b is the width of a fiber tape, t_R and α_R are the thickness of the layer and the initial winding angle on the cylindrical part, respectively. The parameters r_b and r_{2b} are the radius at one and two tape-width distances, respectively, from the turn-around point, and A, B, C and D the four coefficients of the method presented in [3] and defined using boundary conditions (pseudo-ply thickness at the turn-around radius, continuity of the thickness and the curvature in r_{2b} between Eqs. 3 and 4, and constant material volume between r_{turn} and r_{2b}).

2.3 Lay-up determination

In the multi-sequence lay-up of a dome, prediction is a tricky process, given that the determination of both winding angle and thickness is based on the current supporting surface topology, which, in a multi-layer lay-up, depends on the previous supporting surface topologies. The classical process presented by Leh [5] is as follows:

- recovery and storage in internal variables of geometric data (in the form of elliptical liner definition parameters) and winding sequence parameters,
- a definition of the coordinates according to z and r and a discretization of this geometry,
- the calculation of first and second derivatives of current shape line by the finite difference method to solve Eq. 1,
- the resolution of Eq.1 by a Runge-Kutta method to order 4 in order to obtain the value of the radius at the turn-around of the current layer,
- the calculation of the overthickness to be applied to the previous layer thanks to the Wang's formulation,
- normal calculation and application of the previously determined overthickness at each integration point,
- smoothing of new points calculated by a B-spline,
- the looping of all these steps for each layer described by the sequence of the winding angles.

The operation of the routine can be schematized according to the graph of Fig. 2.

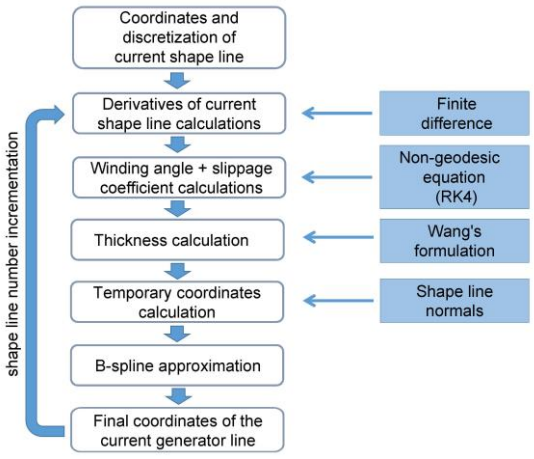

Figure 2. General dome lay-up calculation algorithm

This process has some limitations not compatible with configuration extensions. Thus the tool is not able to deal with winding lay-up other than increasing initial winding angle lay-up. It consequently does not make possible to cover a layer *n* with the layer *n* + 1. It is also highly unstable when covering a convex shape. As shown in Fig. 3, if the integration step is too large, there is a possibility that the normals at two (or more) integration points intersect.

This results in the creation of points for the new layer that will no longer be ordered in an increasing *z* when the overthickness is added.

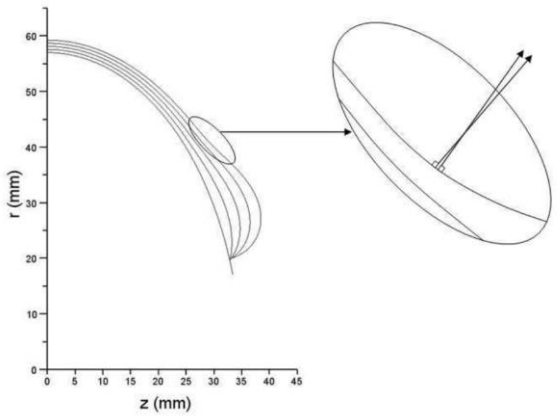

Figure 3. Overlap instability for convex areas due to the interweaving of normals close to integration points

Finally, another critical point consists in the absence of possibility to model the covering of the barrel of the boss by several layers of composite. Indeed this routine foresees that only the first layer reaches the barrel of the boss. Then, because only sequences of increasing winding angles are managed, the other layers can only be modelled with increasing radii at the turn-around point.

3. IMPROVEMENTS

3.1 Digital processing of the evolution of $d\alpha/dz$

All the identified authors use the Runge-Kutta algorithm at order 4 (RK4) to solve Eq. 1 for determining the radius at the turn-around point of the current layer. The main problem with this resolution method is it is highly dependent on the number of integration points resulting from the geometric discretization of the current layer.
As we can see in Fig. 4, the problem is strongly non-linear: the closer we get to $\alpha = 90°$, the more the influence of the discretization step is preponderant. This is problematic because the calculation error via RK4 is strongly related to discretization and consequently to calculation time. The resolution model should also be validated by optimizing the calculation step to reach a cumulative error below an admissible threshold.

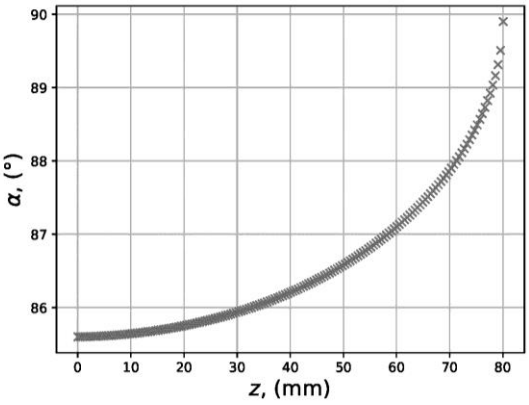

Figure 4. Winding angle variation α according to z

Eq. 1 is an equation whose sensitivity to parameters makes it difficult to solve by explicit numerical methods. The closer we get to $\alpha = 90°$ the more sensitive it is and the less relevant the RK4 algorithm is to solve it. Works using this algorithm do not quantify the error associated with the resolution of this problem with this method. The solution to enable the algorithm to converge is then to define an extremely fine step without obtaining information on the cumulative error. There are many powerful resolution algorithms, originally optimized to run on low-performance machines, alternative to explicit methods.
This is the case with the LSODA [9] algorithm, which offers many advantages. The first is that it is able to manage different resolution methods in the same calculation. Thus, it can switch from an Adams method to a BDF method automatically depending on the degree of stiffness of the differential equation. The algorithm is also independent of the calculation step imposed. The code automatically manages the step needed to solve the problem based on the calculated error to ensure convergence. Once solved on the number of steps strictly necessary, the function then re-interpolates at the integration points specified initially.

3.2 Instabilities due to convex zones

Due to the reduction in the number of integration points compared to a purely explicit routine, the code is then sensitive to the problem of overlapping instability of convex areas (Fig. 3) : physically meaningless loops may appear (Fig. 5a, Fig. 5b). It is therefore necessary to introduce a specific function to erase these loops (Fig. 5b). This function detects each segment consisting of two successive integration points intersecting another segment of the original curve. In order to limit the calculation time, the function must only take into account the convex parts of the curve to be checked. The outputs of this function are all the intersection points of the curve as well as two series of *z* and *r* coordinates of the erased instability loops.

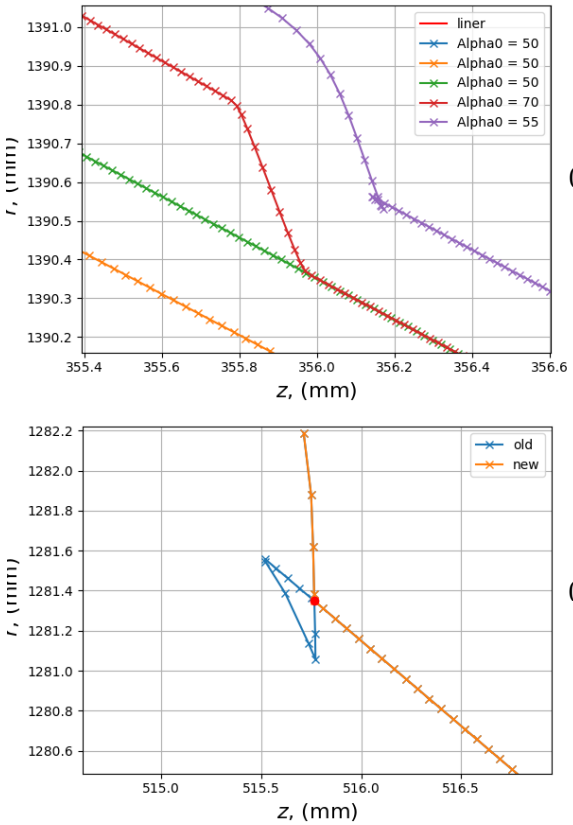

Figure 5. Resolution of instabilities related to convex shapes of geometries for the current layer

In addition, a smoothing function is required to ensure the stability of the next layer simulation (Fig. 6). The degree of the smoothing function will depend on the geometric dimensions of the wound body and the thickness of the composite layers.

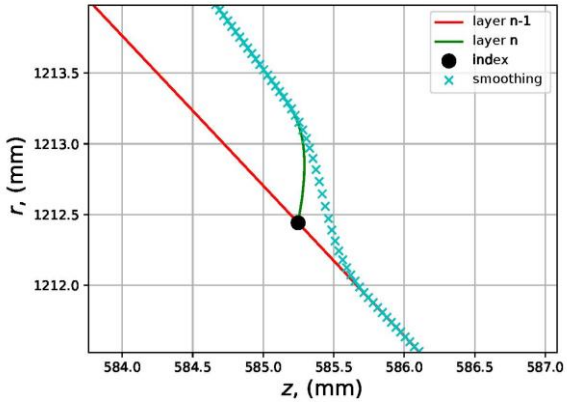

Figure 6. Smoothing of layer n with layer n - 1

This smoothing function has to manage the different possible winding angle sequences:

- sequence with equal initial angles (Fig. 7a),
- sequence with decreasing initial angles (Fig. 7b),
- sequence with increasing initial angles (Fig. 7c),
- sequence with alternation of the three previous types.

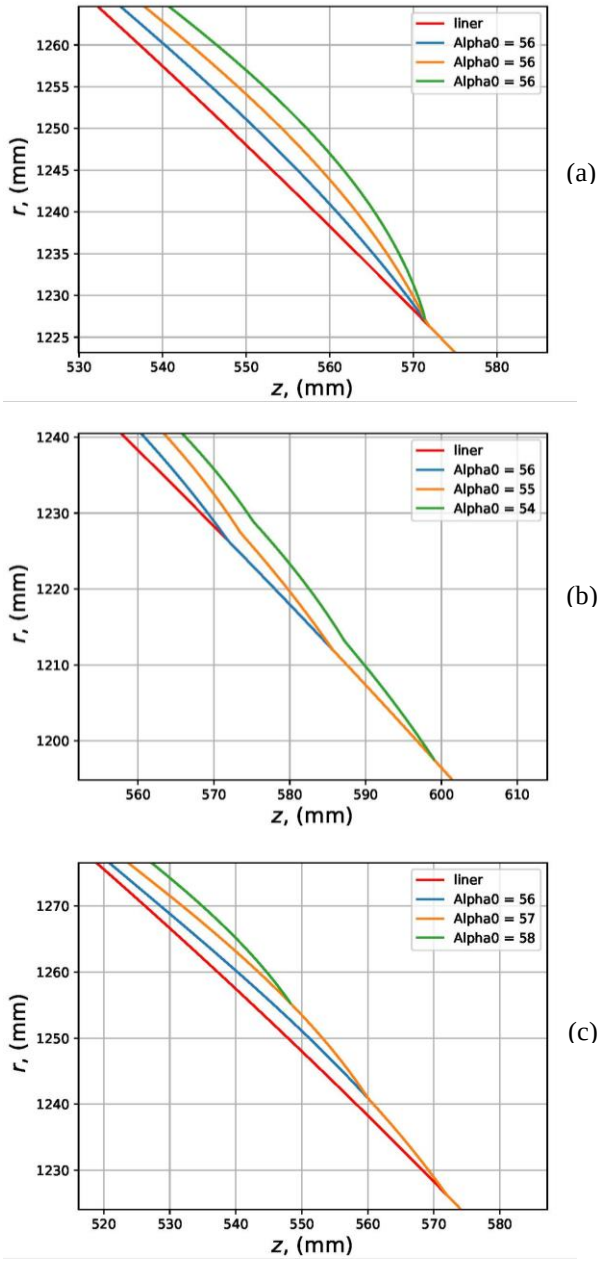

Figure 7. Smoothing routine applied in sequence of equal (a), decreasing (b) and increasing (c) initial winding angles

3.3 Layers overlapping the barrel of the boss

Modelling the helical layers overlapping the barrel of the boss is a development which is less dealt with in the literature, although [10] addresses this issue. In order to take into account these overlappings which may occur near the boss (Fig. 8), a method is proposed to transfer the overthickness. [10] considers a linear extension tangent to the curve at the radius of the boss r_{boss} to be the support for the calculation of the current layer. It then proposes that the volume defined by the winding for $r < r_{boss}$ be reported with respect to the location of

the curve presenting the maximum thickness (r_{tmax}) and satisfying several conditions:

- the thickness is redefined by:

$$t(r) = A + Br + Cr^2 \quad \text{for} \quad r_{boss} \leq r \leq r_{tmax} \qquad (5)$$

- the volume for a radius smaller than r_{boss} is distributed between r_{boss} and r_{tmax},
- continuity of thickness at r_{tmax},
- continuity of slope at r_{tmax}.

Figure 8. Micrograph of storage tanks studied in [10]

The problem with this approach is twofold. First of all, the expression of the thickness in r^2 does not allow to take into account geometries with an inflection point, which is often the case. On the other hand, as can be seen in Fig. 9, this approach does not work if the radius at maximum thickness (r_{tmax}) is also less than r_{boss}.

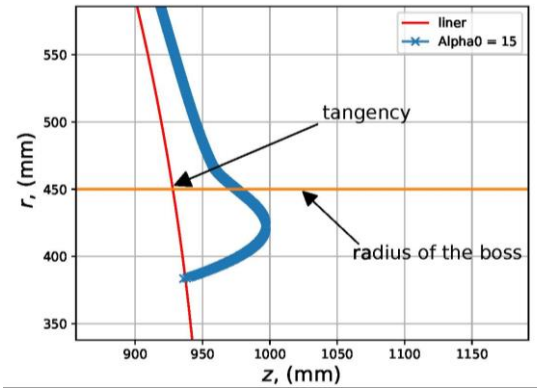

Figure 9. Volume transfer defined by a winding for $r_{turn} < r_{boss}$

A satisfactory routine should be able to handle overlapping layers on the boss. The most common function whose curve has an inflection point is a polynomial function of degree 3. Rather than reasoning about the redefinition of the overthickness to be applied, the geometry of the current layer is directly modified once it has been calculated. It is therefore first necessary to extend the spatial domain of the lower layer which will serve as a support for the calculation of the current layer for the values of $r < r_{boss}$. Note that a second order spline has been finally chosen (Fig. 10a).

As one of the conditions on the polynomial of degree 3 used to smooth this kind of layer regards a volume equivalence, it is necessary to be able to perform a numerical integration. To do this, a polynomial definition of z is chosen as a function of r. A new geometry is then defined as:

$$z = A + Br + Cr^2 + Dr^3 \qquad (6)$$

This new geometry is defined over a transfer length L_{ex}. To determine the parameters A, B, C and D it is necessary to introduce 4 conditions, namely:

- continuity at fixed L_{ex},
- continuity of the slope at L_{ex} ,
- slope equal to the one of previous layer at $r = r_{boss}$,
- conservation of the area between r_{boss} and $r_{boss} + L_{ex}$ for initial formulation and polynomial formulation.

Once the equation system is solved, it is then possible to switch back to a definition of r as a function of z to establish the new geometry. The routine is then able to manage the layers overlapping the barrel of the boss (Fig. 10a) and to propose a redefinition of the geometry in a polynomial of degree 3 (Fig. 10b).

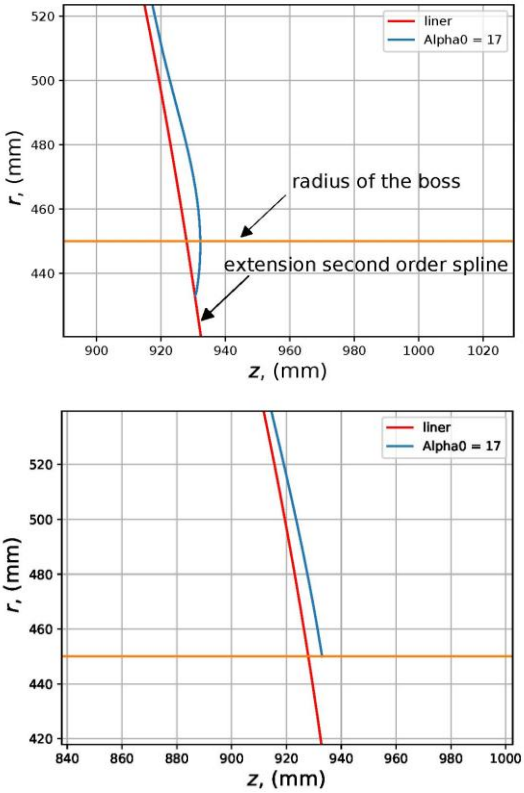

Figure 10. Layer overlapping the barrel of the boss (a) and geometrical definition in the form of polynomial of degree 3 (b)

From a physical point of view, the only value that the winding angle can take in the vicinity of the boss end is $\alpha = 90°$. This corresponds to the tilting of the fiber during winding at the radius at the turn-around point. Indeed, a value lower would mean that the winding head hits the boss barrel.

If the initial winding angle at the cylinder/dome junction is fixed by the process, there is only one parameter left to ensure these conditions, *i.e.* λ. This parameter is then optimized to ensure that the winding is feasible. To do this, the routine solves Eq. 1 backwards from the radius at the turn-around point $r_{turn} = r_{boss}$ with a definition of λ set by a value of λ_{max}. The idea is then to compare the value of the calculated initial winding angle with the value of the imposed initial winding angle and this by modifying the value of the parameter λ_{max} during optimization process.

For this one must defined a cost function:

$$\Delta = \alpha_0(\lambda_{max}) - \alpha_0 \tag{7}$$

Thanks to an adapted algorithm, it's possible to optimize this calculation by minimizing this cost function, i.e. by searching for the root of:

$$\Delta = 0, \quad -\mu_s < \lambda_{max} < \mu_s \tag{8}$$

where μ_s is the static friction coefficient, the maximum value of the sliding coefficient beyond which it becomes impossible to wind.

Thus it is possible to identify the λ_{max} value that satisfies both $\alpha = \frac{\pi}{2}$ at the barrel of the boss and $\alpha = \alpha_0$ for $r = R$.

4. CONCLUSION

The work presented here allows the development of a generic filament winding routine to simulate any sequence. It is not limited to specific geometries (which must be axisymmetric) and is suitable to any winding sequence. This is made possible by a number of functions developed such as smoothing or winding stabilization functions on convex geometries. Particular attention is paid to a physical interpretation of certain parameters such as the definition of the slip coefficient or the management of the winding angle in the vicinity of the boss.

The interest of this approach is to propose the integration of a simulation module of the winding process, flexible enough to be adaptable to the geometrical peculiarities of the motor cases or tanks, in a design and optimization tool for wound composite structures sizing.

Acknowledgments

This research is supported by the French Space Agency (CNES).

5. REFERENCES

1. Vasiliev V., Krikanov A. & Razin A. (2003). New generation of filament-wound composite pressure vessels for commercial applications. *Compos. Struct.* **62**(3–4), 449–59.
2. Koussios S. & Beukers A. (2008). Influence of laminate thickness approximation methods on the performance of optimal filamentary pressure vessels. *23rd Annual Conference of the American Society for Composites, Memphis, TN*.
3. Wang R., Jiao W., Liu W. & Yang F. (2010). A new method for predicting dome thickness of composite pressure vessels. *J. Reinf. Plast. Compos.* **29**(22), 3345–52.
4. Wang R., Jiao W., Liu W. & Yang F. (2011). Dome thickness prediction of composite pressure vessels by a cubic spline function and finite element analysis. *Polym. Polym. Compos*. **19**(2-3), 227–34.
5. Leh D., Saffré P., Francescato P. & Arrieux R. (2013). Multi-sequence dome lay-up simulations for hydrogen hyper-bar composite pressure vessels. *Composites Part A: Applied Science and Manufacturing*, **52**, 106–17.
6. Carvalho J.D., Lossie M., Vandepitte D. & Brussel H.V. (1995). Optimization of filament wound parts based on non-geodesic winding. *Compos. Manuf.* **6**(2), 79–84.
7. Zu L., Koussios S. & Beukers A. (2010). Design of filament-wound domes based on continuum theory and non-geodesic roving trajectories. *Composites Part A: Applied Science and Manufacturing.* **41**(9), 1312–20.
8. Kim C.U., Kang J.H., Hong C.S. & Kim C.G. (2005). Optimal design of filament wound structures under internal pressure based on the semi-geodesic path algorithm. *Compos. Struct.* **67**(4), 443–52.
9. Brown P.N. & Hindmarsh A.C. (1989). Reduced storage matrix methods in stiff ODE systems, *Applied Mathematics and Computation*. **31**, 40-91.
10. El Moussaïd M. (2016). Analyse et intégration des spécificités liées au procédé de fabrication dans les modèles de calcul des structures composites. Application à la simulation du comportement mécanique des fonds des réservoirs bobinés. *PhD thesis.*